

Influence of Complexing Agents on the Structure and Electrochemical Properties of $\text{LiNi}_{0.80}\text{Co}_{0.15}\text{Al}_{0.05}\text{O}_2$ Cathode Synthesized by Sol-Gel Method: a Comparative Study

Peng Dong^{1,2,*}, Shu-biao Xia^{1,2,3}, Ying-Jie Zhang^{1,2}, Yan-nan Zhang^{1,2}, Zhen-ping Qiu^{1,2}, Yao Yao^{1,2}

¹ Faculty of Metallurgical and Energy Engineering, Kunming University of Science and Technology, Kunming 650093, China.

² Engineering Laboratory for Advanced Batteries and Materials of Yunnan Province, Kunming 650093, China.

³ Chemistry of Functional Materials and Pollution Control Research Center, Qujing Normal University, Qujing 655011, China.

*E-mail: dongpeng2001@126.com.

Received: 18 October 2016 / Accepted: 14 November 2016 / Published: 12 December 2016

A comparative study refers to textural and electrochemical properties of different Li-ion battery $\text{LiNi}_{0.80}\text{Co}_{0.15}\text{Al}_{0.05}\text{O}_2$ cathode materials (denoted as NCA; being prepared by the sol-gel method using EDTA, glycine and citric acid as complexing agents) have been reported in this work. The textural properties of the as-prepared samples were characterized by scanning electron microscopy (SEM), transmission electron microscopy (TEM) and powder X-ray diffraction (XRD). Characterization results display that the resultant NCA-EDTA cathode shows the best structural integrity, the best layer structure, and the largest lattice spacing. The initial discharge capacity of the NCA-EDTA electrode synthesized by using EDTA as complexing agents is much larger than those for NCA-glycine and NCA-citric acid. Meanwhile, the resultant NCA-EDTA cathode also exhibits more excellent cycle ability than those of NCA-glycine and NCA-citric acid. In addition, compared with NCA-glycine and NCA-citric acid samples, the NCA-EDTA still shows the largest Li^+ diffusion coefficient. All these advantages related to the electrochemistry may come down to the structural advantages of the NCA-EDTA under the assistant of EDTA in the synthesis processes.

Keywords: $\text{LiNi}_{0.80}\text{Co}_{0.15}\text{Al}_{0.05}\text{O}_2$; citric acid; EDTA; glycine; the comparative study

1. INTRODUCTION

Among currently available energy storage technologies, the rechargeable lithium ion battery (LIB) has received considerable attention from both the academic community and industry as a power source for hybrid electric vehicles (HEVs) and portable electronic devices due to its long cycle life and

high energy density [1,2]. With Tesla pure electric vehicles hotting in the global market, the use of Panasonic 18650 battery has attracted widespread attention; in which, the $\text{LiNi}_{0.80}\text{Co}_{0.15}\text{Al}_{0.05}\text{O}_2$ (denoted as NCA) material with very high energy density were used cathode material. In detail, its rated capacity is 3400 mAh, being much larger than the general 18650 batteries exist in the market that just has a rated capacity of 2600 mAh. NCA cathode materials are high-nickel ternary material, which is usually synthesized by conventional solid-phase sintering and co-precipitation methods [3]. However, in the existing methods for prepared NCA cathode materials, uniformly mixing the raw materials and mixing lithium appear bottlenecks, thus causing a negative impact on the performance of NCA [4]. In a solid-phase method, when precursors are sintered between 700-800 °C, Al^{3+} is difficult to form an excellent solid solution structure. On the other hand, upon the co-precipitation under alkaline conditions, the appeared $\text{Al}(\text{OH})_3$ will dissolve into AlO_2^{-1} , which is also deadly for synthesizing excellent NCA cathode materials [5].

C J Han et. al. have synthesized NCA cathode materials by a sol-gel method [6], results show that the resultant $\text{LiNi}_{0.8}\text{Co}_{0.2-x}\text{Al}_x\text{O}_2$ samples show the typical $\alpha\text{-NaFeO}_2$ Layered structure when $x \leq 0.05$. Specially, with increasing Al content in the cathode materials, capacity of retention rate has increased for $\text{LiNi}_{0.8}\text{Co}_{0.2-x}\text{Al}_x\text{O}_2$; nevertheless, the initial discharge capacity of $\text{LiNi}_{0.8}\text{Co}_{0.2-x}\text{Al}_x\text{O}_2$ with a high x value decreases slightly. Previous experimental results tell us that sol-gel method can effectively solve the problems appeared in Al-doping; however, many factors affect the performance of NCA material prepared by the sol-gel process, such as solvents, complexing agents, pH of solutions, and other reasons impacting structures of materials [7,8]. Among them, complexing agents used for preparing NCA material is fairly important but always reflected by the complexation between the complexing agents and transition metal ions [9,10]. The difference in the complex efficiency of different complexing agents/the transition metal ion and the difference of complexing constants of different complexing agents all result in different reactions during the hydrolysis rate [11]. These differences will influence the distribution of elements and materials particle size in the materials, and then impact the structural and electrochemical properties of resultant material [12]. At the same time, by using different complexing agents, the synthesis time is not the same for forming a dry gel [6].

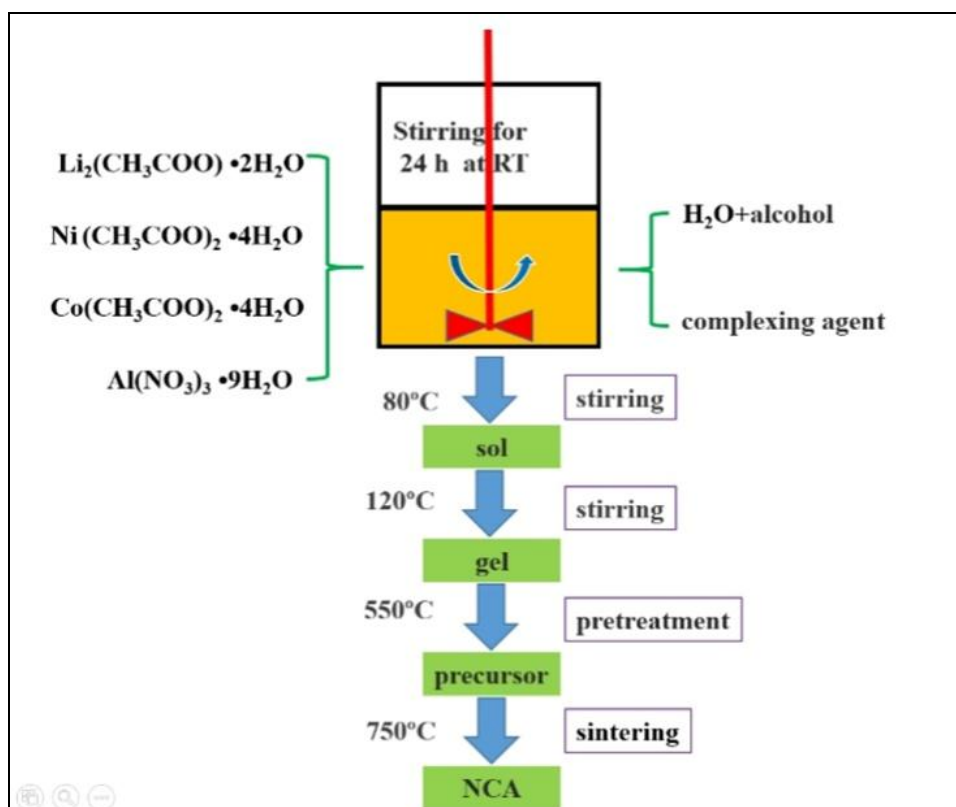
With these in mind, in this paper, we attempt to use several common organic complexing agents (such as EDTA, Glycine and citric acid) for preparing different NCA cathodes by a sol-gel method; in addition, we expect to explore the effect of complexing agents on the structural and electrochemical properties of resultant materials.

2. EXPERIMENTAL

Scheme 1 shows a flow chart for preparing NCA cathode materials by sol-gel method. Stoichiometric amounts of $\text{Li}_2(\text{CH}_3\text{COO})\cdot 2\text{H}_2\text{O}$, $\text{Al}(\text{NO}_3)_3\cdot 9\text{H}_2\text{O}$, $\text{Co}(\text{CH}_3\text{COO})_2\cdot 4\text{H}_2\text{O}$, $\text{Ni}(\text{CH}_3\text{COO})_2\cdot 4\text{H}_2\text{O}$ were dissolved in solvent which mixed deionized water and ethanol. The mixed solution was formulated of 0.5 mol L^{-1} total concentration of metal ion. EDTA, citric acid and glycine as complexing agent were fixed to be 1: 1. The mixed solution was stirred at room temperature for 24 h and then transferred into the oil bath at 80 °C with stirring for 4 h to form a uniform sol. Finally the

sol was dried to form a dry gel at 120 °C by controlling the stirring speed. The dry gel was heated with a heating rate of 2 °C min⁻¹ and decomposed at 550 °C for 6 h. The powders were calcined at 800 °C for 24 h in oxygen and then the sample was cooled slowly in the furnace to room temperature. In order to probe the morphologies and structural constituents of resultant samples, we have adopted the FE-SEM (Shimadzu, Japan) and JEOL 3011 microscope (which works at an operating voltage of 300 keV by using the Lab6 filament) for collecting the electron electronic speculum images of each as-prepared sample. Meantime, X-ray diffraction (XRD) patterns were also performed using the Rigaku D/max2200 (Cu-K- α radiation, 40 kV, Rigaku) for determining the phase of resultant samples.

On the other hand, for realizing the follow-up electrochemical experiments, we first mixed 85 wt.% of NCA, 8 wt.% of PVDF, and 7 wt.% of carbon black into the appropriate quantity of N-methyl pyrrolidinone (NMP) solvent. Following closely, they are uniformly daubed onto the clean aluminum foil and then dried for at 80 °C in a vacuum drying oven 12 h. In order to assemble the batteries, Coin-type cells (CR 2025) were used; meanwhile, lithium metal foil, 1.0 M LiPF₆ solvent (EC: DEC: DMC = 1: 1: 1 in volume ratios) and NCA/PVDF/carbon black modified aluminum foil were used as the anode, electrolyte and cathode, respectively. The charged and discharged tests of as-prepared cells were carried out between the current densities of 0.2-5 C and simultaneously between 2.75-4.3 V for comparing the electrochemical behaviors of resultant NCA cathode materials prepared with different complexing agents. Cyclic voltammetry (CV) was operated on an Autolab electrochemical workstation (PGSTAT-302n, Netherlands) at a scan rate of 0.1 mV s⁻¹ between 2 V-4.8 V.



Scheme 1. Flowchart for the synthesis of NCA cathode by Sol-gel method.

3. RESULTS AND DISCUSSION

Figure 1 shows the SEM images for NCA-EDTA, NCA-Glycine, and NCA-Citric acid cathodes synthesized by using different complexing agents. One can see that the secondary particle for NCA-EDTA, NCA-Glycine, and NCA-Citric acid all have irregular morphologies and broad size distributions (the sizes of the secondary particles are all less than 10 μm). Figure 1 a1-a3 illustrates the morphology of NCA-EDTA under three different magnifications. As can be seen, the secondary particles composed of fine NCA particles are perfect. No small nano size particles or octahedral structures have appeared in the SEM images. However, for the NCA-Glycine, the secondary powder consists of loose fine particles with nano size adherents on the rounded particle surface can be clearly observed (Figure 1 b1-b3). Specially, when sintering at 800 $^{\circ}\text{C}$, smaller primary particles will melt to form a small number of new octahedron structures by re-crystallization. This also laterally demonstrates that when using glycine as complexing agent, the primary particles of resultant NCA-Glycine sample are smaller because of the complex effect of glycine to metal are weaker than EDTA. Thus, the complex particles cannot grow up rapidly. In fact, the existence of the octahedral structures is not conducive to electrochemical performance of NCA material [13]. At last, for the NCA-Citric acid sample, the situation becomes worse (as shown in Figure 1 c1-c3). The structures of most secondary powder have cracked into small particles with the sizes less than 1 μm , what's worse is that almost each primary particle displays the typical octahedral structures. Seeing from the SEM images, one can see that NCA-EDTA shows the best structural integrity because of the super complexing ability between EDTA and metal atoms. The crystal structure of the NCA-EDTA, NCA-Glycine, and NCA-Citric acid particles were investigated by XRD and shown in Figure 2. There is no any impurity phase has been detected, the resultant NCA-EDTA, NCA-Glycine, and NCA-Citric acid samples all correspond to the layered $\alpha\text{-NaFeO}_2$ structure (space group, R-3m). Specially, the separations of 018/110 peaks in the XRD spectra also represent the layered character of structure and simultaneously demonstrate the good electrochemical properties of samples.

Lattice parameters shown in Table 1 are obtained by the least squares method of unit cell parameters. As can be seen, NCA-EDTA particles show the largest c/a value and I_{003}/I_{104} values. The NCA-EDTA particles display the minimum lattice parameter along the a-axis but the maximum lattice parameter along the c-axis. The incorporation of the smaller and more polarizing Al^{3+} and Co^{3+} ion in place of the larger Ni^{2+} ion is the reason for the decreases of a value [14]. The increases of c parameter could due to the polarizing effect of the Al^{3+} ion in the $[\text{MO}_2]$ layers, which will distort the structure and increase the interlayer distance along c-axis. Meanwhile, its c/a ratio is also the largest, which is due to the substitution of Al ions in the locations of Ni or Co ions and to the ionic character of the Al-O bond [6]. Table 2 shows that several elements in NCA material with different valence ionic radius. The main reason for this result is the uniform distribution of the precursor element and particle size distribution so that the oxidation strength of solid-phase reaction is improved. Because the EDTA complexation ability is the strongest, so the most stable complex was produced [15].

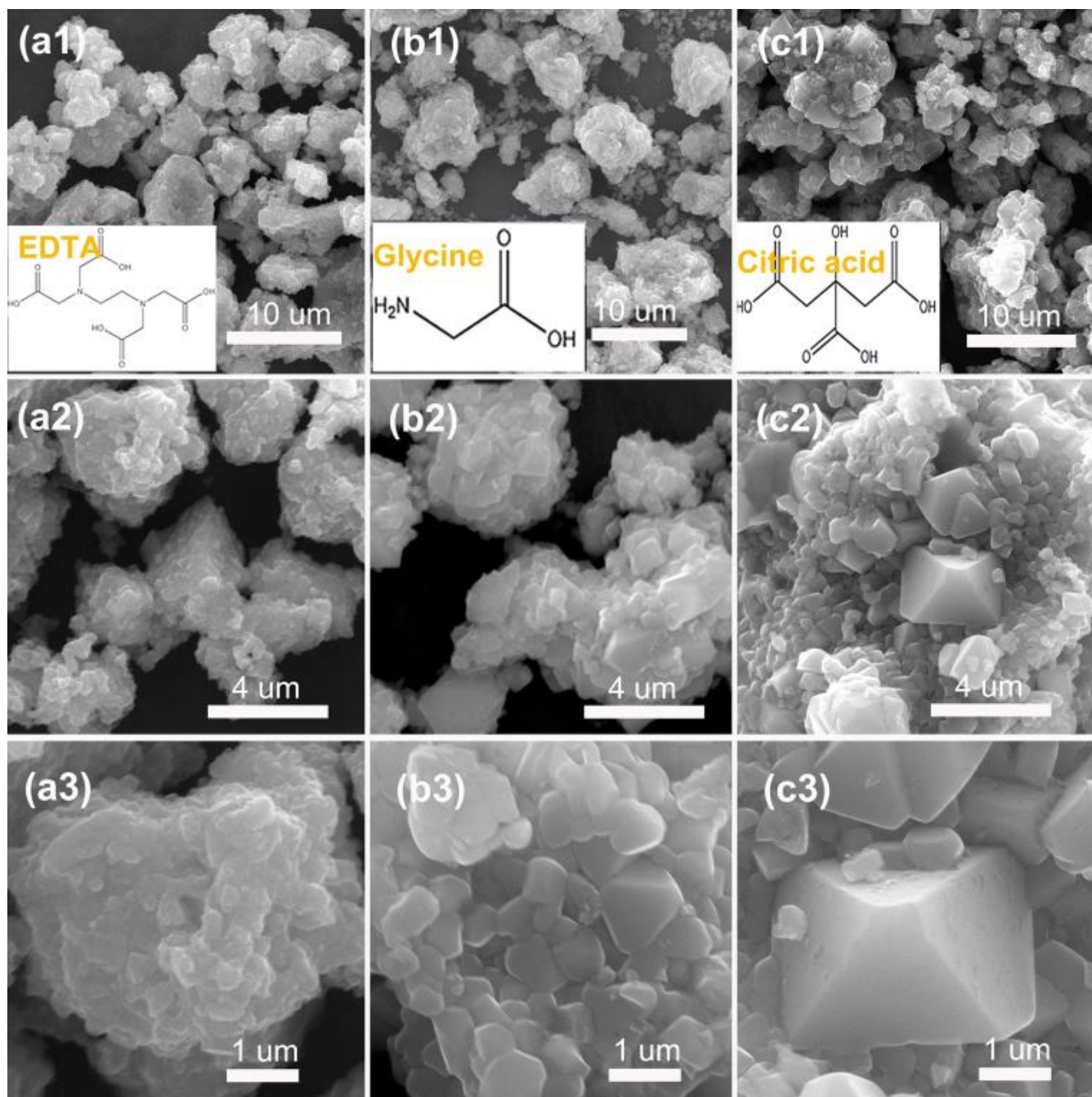


Figure 1. SEM images of NCA cathodes prepared by different complexing agents: (a1-a3) NCA-EDTA, (b1-b3) NCA-Glycine, and (c1-c3) NCA-Citric acid.

For deeper understanding the microstructures of NCA-EDTA, NCA-Glycine and NCA-Citric acid particles, their TEM and HRTEM images have been recorded in Figure 3. As shown in Figure 3 a1, the TEM image of marginal part of NCA-EDTA particles displays that the edges of each small particles are close to rounded. Meanwhile, all small particles compactly pack. This kind of structure is conducive to the long-term stability of electrochemical activity for NCA-EDTA. However, similar to the SEM image, TEM image of NCA-Glycine (Figure 3 b1) also shows that the secondary powder consists of loose fine particles with nano sized adherents on the rounded particle surfaces. Specially,

TEM image displays the typical sharp edges of NCA-Glycine (Figure 3 c1), once again proves the appearing of typical octahedral structures. On the other hand, HRTEM images (Figure 3 a2-c2) of NCA-EDTA, NCA-Glycine, and NCA-Citric acid particles demonstrate that lattice spacing values decrease by the order of NCA-EDTA (3.9 Å) > NCA-Glycine (3.7 Å) > NCA-Citric acid (3.1 Å). The largest lattice spacing value indicates the best layered structure of NCA-EDTA than NCA-Glycine and NCA-citric acid.

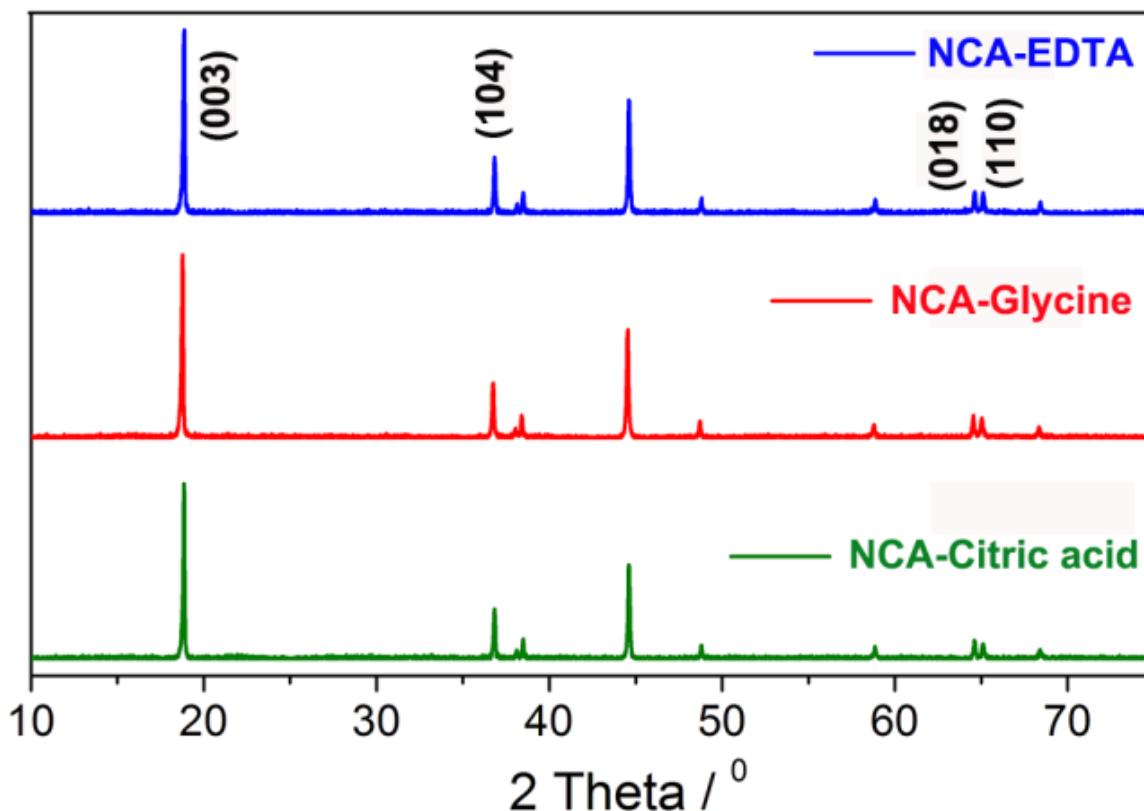


Figure 2. XRD patterns of NCA-EDTA, NCA-Glycine, and NCA-Citric acid cathodes prepared by using different complexing agents.

Table 1. Lattice parameters of NCA-EDTA, NCA-Glycine, and NCA-Citric acid cathodes prepared by using different complexing agents.

	a (Å)	c (Å)	c/a	I_{003}/I_{104}	V (Å ³)
EDTA	2.8664	14.1722	4.944	1.684	100.84
Glycine	2.8695	14.1050	4.915	1.629	100.58
Citric acid	2.8691	14.1122	4.919	1.660	100.60

At last, one can see from 003 planes of NCA-citric acids (Figure 3 c2) that a large number of crystal defects and intergranular blurred appeared in NCA-citric acids. All these results demonstrate that the NCA-EDTA cathode own the best crystal structures and the best structural integrity than other homologous NCA cathodes because of the advantages of EDTA complexing agents.

Table 2. Ionic radius of several elements in NCA cathode.

	Ni ²⁺	Ni ³⁺	Ni ⁴⁺	Co ²⁺	Co ³⁺	Co ⁴⁺	Al ³⁺	Li ⁺	O ²⁻
Å	6.9	5.6	4.8	7.45	5.45	5.3	5.35	7.6	14

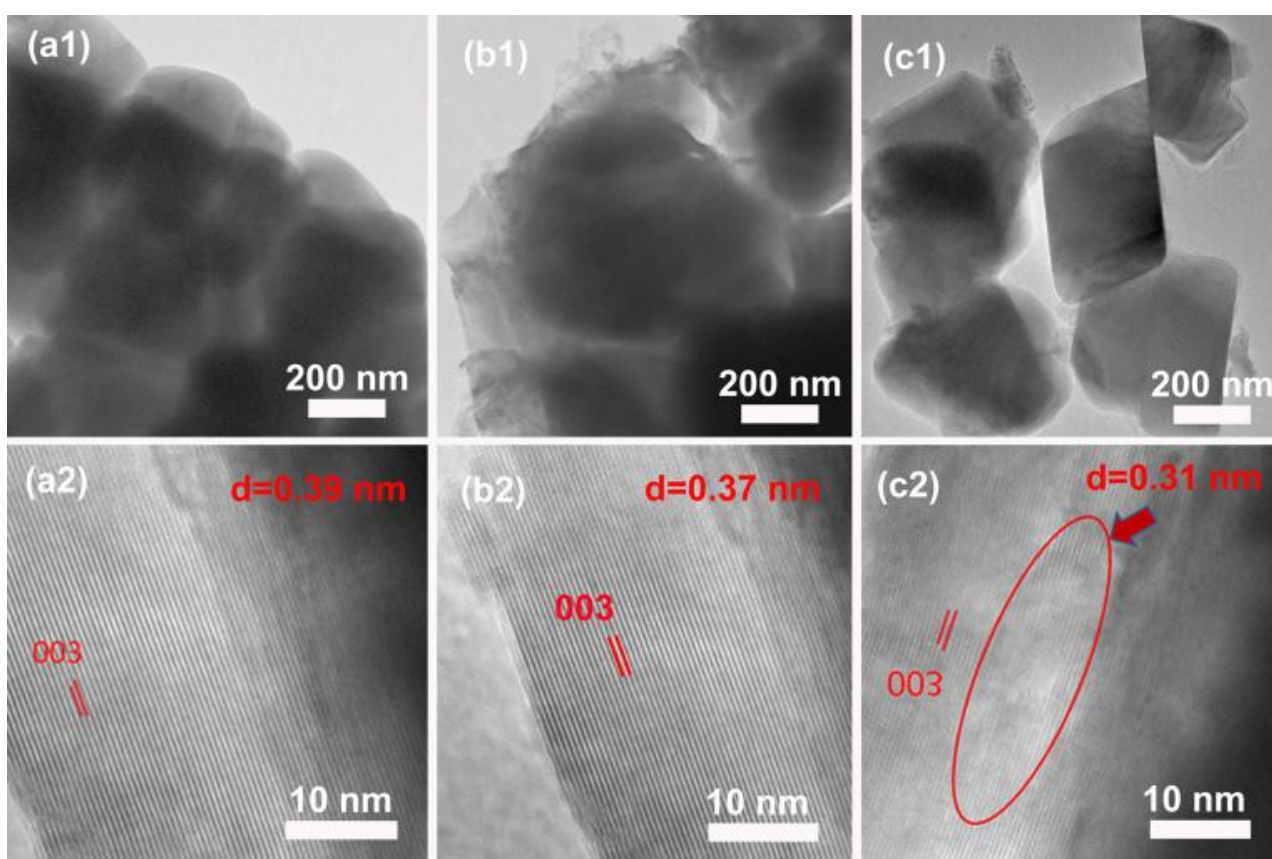


Figure 3. TEM (a1-c1) and HRTEM (a2-c2) images of NCA-EDTA cathode(a1, a2), NCA-Glycine (b1, b2), and NCA-Citric acid cathode (c1, c2) prepared by using different complexing agents.

Figure 4 and Figure 5 shows the initial charge/discharge curves and cycling performances of NCA-EDTA, NCA-Glycine, and NCA-Citric acid samples prepared by using different complexing agent at different 0.2 and 1 C, respectively. At 0.2 C (Figure 4a), NCA cathode materials obtained initial discharge capacity values of 175.1 mAh g⁻¹, 168.9 mAh g⁻¹ and 162.7 mAh g⁻¹ corresponding to NCA-EDTA, NCA-glycine and NCA-citric acid, respectively. Meanwhile, after 30 cycles, the capacity retention rate was 97.3%, 96.6% and 94.4% for NCA-EDTA, NCA-glycine and NCA-citric acid

cathodes, respectively (Figure 5a). At 1 C (Figure 4b), their initial discharge capacity was 159.8 mAh g⁻¹, 153.8 mAh g⁻¹ and 141.1 mAh g⁻¹ corresponding to NCA-EDTA, NCA-glycine and NCA-citric acid cathodes, respectively. However, their capacity retention values are 92.3%, 80.7% and 87.8% for NCA-EDTA, NCA-glycine and NCA-citric acid after 50 cycles, respectively (Figure 5b). According to the above test results, using different complexing agents has a greater impact on the electrochemical performances of NCA material prepared by sol-gel method. When using EDTA as the complexing agent, NCA-EDTA shows the best initial discharge capacity and cycle capacity retention rate.

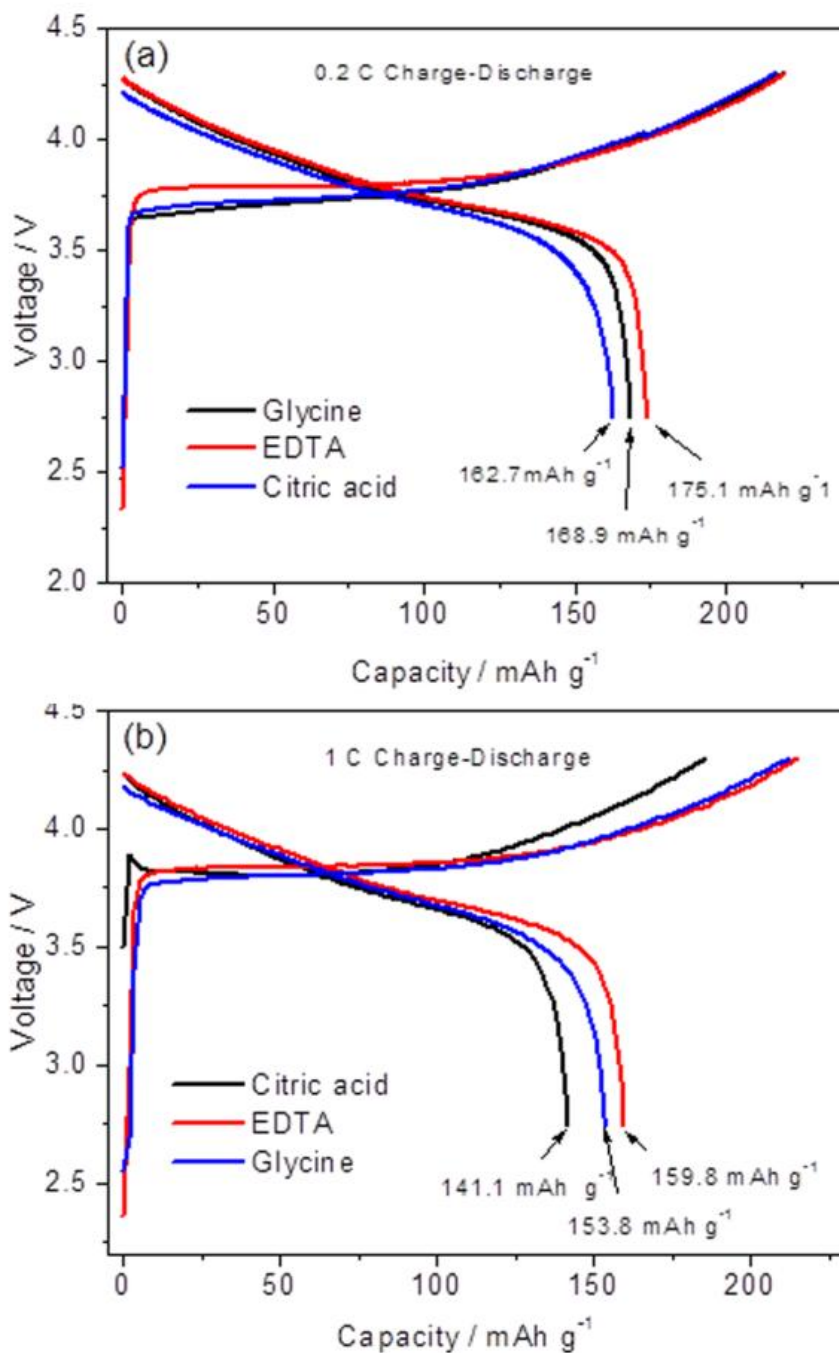


Figure 4. The initial charge-discharge curves of NCA-EDTA, NCA-Glycine, and NCA-Citric acid cathodes recorded at 0.2 C (a) and 1 C (b).

We also make comparison between our NCA-EDTA, NCA-glycine and NCA-citric acid cathode materials with other similar cathode materials for lithium ion batteries that were described in literature. As shown in Table 3, our optimal NCA-EDTA cathode displays similar initial discharge capacity value but better capacity retention value to the NCA cathode synthesized by the solid-state method [16-18]. Specially, when comparing with the NCA cathode prepared with the typical co-precipitation method [19-21], the optimal NCA-EDTA cathode material shows not only the better initial discharge capacity value, but also the much better cycling stability. More recently, vast study have proved that coating NCA with a stable layer (such as: inactive metal oxide $ZrO_2/V_2O_5/SiO_2$, metal fluoride, and metal phosphate) is another effective way to enhance its electrochemical and thermal properties. Herein, when comparing with the TiO_2 or CeO_2 -coated NCA cathodes [22-24], although our optimal NCA-EDTA cathode material shows slightly worse initial discharge capacity value, it displays better cycling stability. Even though comparing with the commercial NCA cathode [25], it still shows the better stability. All these results once again demonstrate that the best structural integrity, the best layer structure, and the largest lattice spacing of the optimal NCA-EDTA cathode contribute to not only the discharge capacity, but also the capacity retention values.

Table 3. Comparison of cell parameters of NCA-EDTA, NCA-Glycine, and NCA-Citric acid cathodes to other reported samples.

Samples	Initial discharge capacity values at 0.2 C ($mAh\ g^{-1}$)	Capacity retention values at 0.2 C (%)	Reference
$LiNi_{0.80}Co_{0.15}Al_{0.05}O_2$ -EDTA	175.1	97.3	This Work
$LiNi_{0.80}Co_{0.15}Al_{0.05}O_2$ -Glycine	168.9	96.6	
$LiNi_{0.80}Co_{0.15}Al_{0.05}O_2$ -Citric acid	162.7	94.4	
$LiNi_{0.80}Co_{0.15}Al_{0.05}O_2$ (solid-state)	178.2	91.6	[16]
$LiNi_{0.80}Co_{0.15}Al_{0.05}O_2$ (solid-state)	180.4	87	[17]
$Li_{1+z}Ni_{0.80}Co_{0.15}Al_{0.05}O_2$ (solid-state)	170-174	<90	[18]
$LiNi_{0.8}Co_{0.15}Ti_{0.05}O_2$ (co-precipitation)	136	82	[19]
$LiNi_{0.8}Co_{0.15}Ti_{0.05}O_2$ (co-precipitation)	174.2	86.7	[20]
$LiNi_{0.80}Co_{0.15}Al_{0.05}O_2$ (co-precipitation)	178.3	90.24	[21]
CeO_2 -coated $LiNi_{0.8}Co_{0.15}Al_{0.05}O_2$	182	86	[22]
CeO_2 -coated $LiNi_{0.8}Co_{0.15}Al_{0.05}O_2$	184	86	[23]
TiO_2 -coated $LiNi_{0.8}Co_{0.15}Al_{0.05}O_2$	192	63.5	[24]
$LiNi_{0.8}Co_{0.15}Al_{0.05}O_2$ (commercial)	187.7	85.1	[25]

Figure 6 shows the CV curves of NCA-EDTA, NCA-glycine and NCA-citric acid cathodes. According to the CV curves, the diffusion coefficient of lithium ions for NCA-EDTA, NCA-glycine and NCA-citric acid cathodes have been calculated and shown in Table 3. Suppose lithium ion de-intercalation process of cathode material is reversible, the electrode is plate electrode, and the system is in line with a semi-infinite diffusion model. According to Randles-Sercik equation deformed at room temperature [26]:

$$I_D = 2.69 \times 10^5 n^{3/2} A \Delta C_0 D_{Li}^{1/2} v^{1/2}$$

Where: n is the number of electrons gains and losses during the reaction, which is 0.59; A is the material surface area of positive electrode involved in the reaction (which is the ratio of surface area to mass multiplied by the positive electrode active material calculated the average specific surface area of the active substance $10 \text{ m}^2 \text{ g}^{-1}$); v is the scan speed of cyclic voltammetry, 0.10 mV s^{-1} ; Co scans before and after the change in the bulk phase of lithium ions, its value and the gains and losses during the reaction electron number and tap density cathode materials related to the vibration of all materials density test value is 1.90 g cm^{-3} , $C_0=0.01166 \text{ mol cm}^{-3}$.

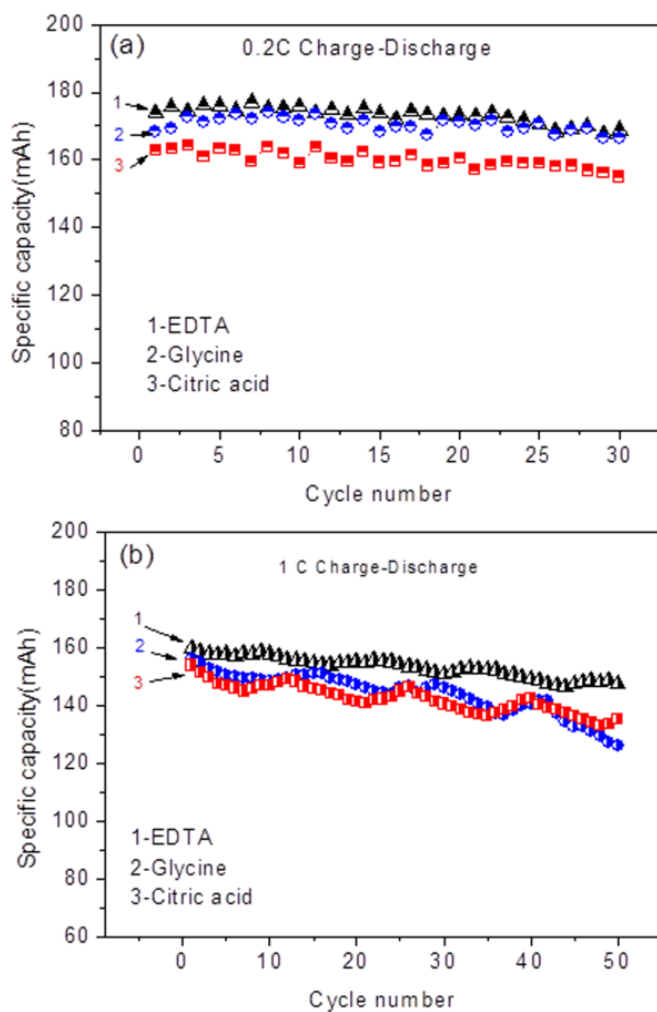


Figure 5. The cycle curves of NCA-EDTA, NCA-Glycine and NCA-Citric acid cathodes recorded at 0.2 C (a) and 1 C (b).

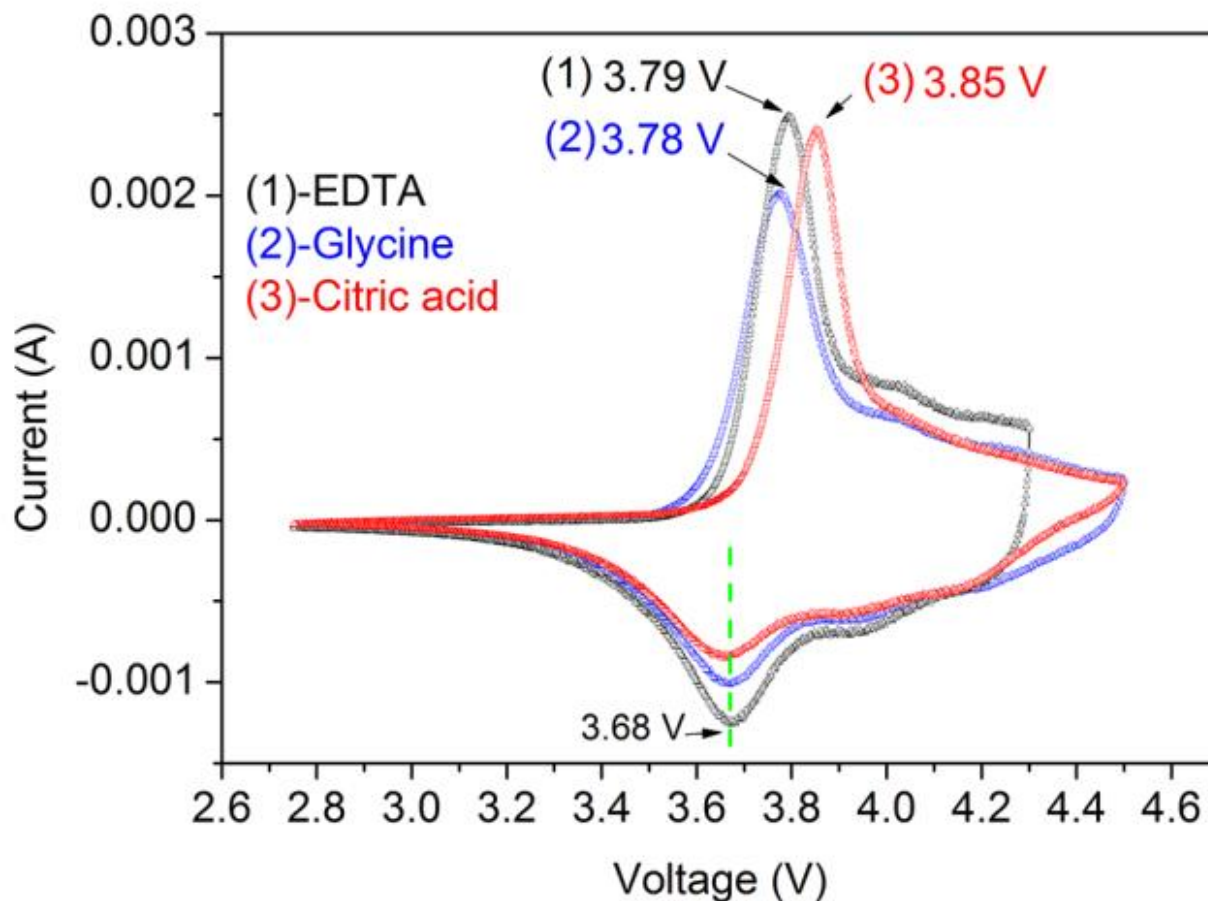


Figure 6. The CV curves of NCA-EDTA, NCA-Glycine and NCA-Citric acid cathodes.

The recorded Lithium ion diffusion coefficients are shown in Table 4, NCA-EDTA shows the largest lithium ion diffusion coefficient. Redox voltage difference of NCA-EDTA is small, indicating its good redox properties. While the NCA-citric acid has the minimum diffusion coefficient, indicating that vast octahedral single crystal structures really affect the de-intercalation distance of lithium ions [27].

In general, the larger stable constants of complexing agent, the more stable complex product; meantime, the rate of hydrolysis reaction will become slow; which can decrease the average particle sizes of precursors and cathode materials. Those small particles will melt and grow along with the recrystallization of crystal grains into the octahedral structure in the solid phase reaction process. As shown in Figure 1c1-c3, vast octahedral structure can further increase the lithium ion de-intercalation distance [28], affect the electrochemical properties of NCA cathode material. One can see from the charge-discharge characteristics curve and cycle performance that NCA-EDTA cathode material displays the best electrochemical properties.

Table 5 shows the physical and chemical properties of several complexing agents. It is clear that the hydrogen bond acceptors and hydrogen bond donors of EDTA, glycine, and citric acid are not the same. At the same time, their complexation stability constants are also different when interacting

with Co^{2+} , Ni^{2+} and Al^{3+} . Specially, the complex stability constant is the largest for EDTA interacting with the metal ion compared with those for both citric acid and glycine complexing agents.

Table 4. The CV data of NCA-EDTA, NCA-Glycine and NCA-Citric acid samples prepared by different complexing agents.

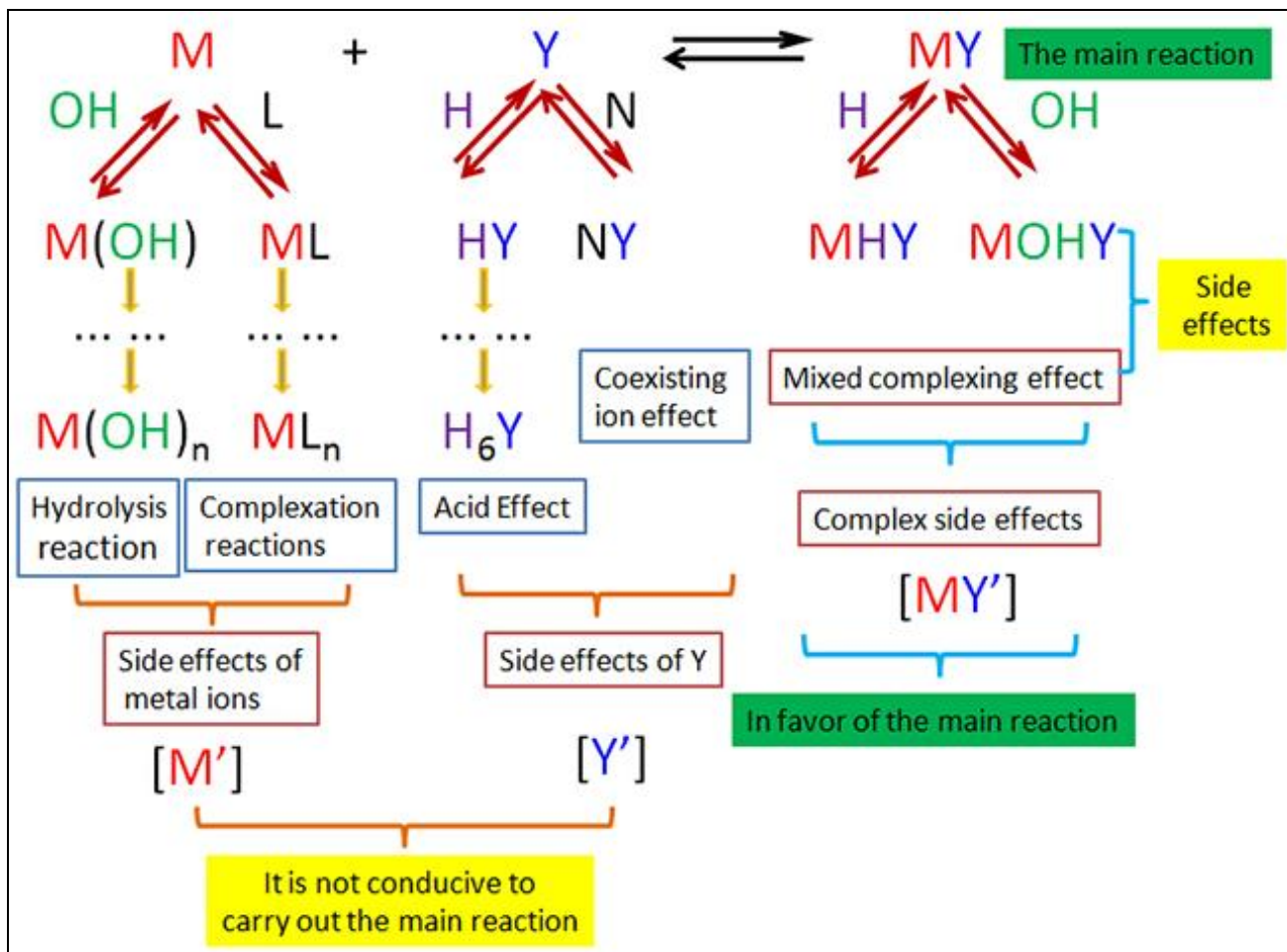
	φ_{pa} (V)	φ_{pc} (V)	$\Delta\varphi_{\text{p}}$ (V)	I_{pa} (mA)	A (cm^2)	D_{Li} (cm^2s^{-1})
EDTA	3.79	3.68	0.11	2.51	65.74	8.11×10^{-11}
Glycine	3.78	3.68	0.10	2.03	79.91	4.34×10^{-11}
Citric acid	3.85	3.68	0.17	2.40	61.24	3.58×10^{-11}

Table 5. Physical and chemical properties of several complexing agents.

	EDTA	Glycine	Citric acid	
Formula	$\text{C}_{10}\text{H}_{16}\text{N}_2\text{O}_8$	$\text{C}_2\text{H}_5\text{NO}_2$	$\text{C}_6\text{H}_8\text{O}_7$	
Molecular weight	292.24	75.07	192.12	
Hydrogen donor number	4	2	4	
Hydrogen receptor number	10	3	7	
Complex stability constant	Al^{3+} 1	4.71	15	
	Co^{2+} 1	5.23		
	Co^{2+} 2	16.1	9.25	13.34
	Co^{2+} 3		10.76	
	Ni^{2+} 1		6.18	
	Ni^{2+} 2	18.56	11.14	15.4
		Ni^{2+} 3	15.00	

Thus, EDTA shows the strongest complexing capacity, but those for glycine and citric acid moderate are weaker. In addition to the impact on the balance of the main reactor complex; the hydroxide precipitation, acid effect, and coexistence ion reaction may also have a greater influence on the rate of complexation reactions. Scheme 2 illustrates a complex of factors influence the reaction equilibrium [29]. The higher $[\text{H}^+]$, smaller $[\text{Y}]$ and smaller $\alpha_{\text{Y}}(\text{H})$ will more severely affect the acid reaction; when the higher $[\text{OH}^-]$ and more $\alpha_{\text{M}}(\text{OH})$, precipitation reaction also become more cruel, the above two cases are not conducive to the main complex reaction carried out [30]. EDTA and citric acid have four hydrogen bond donors, but EDTA owns more hydrogen bond donors. According to the

theory of coordination chemistry, citric acid has the largest complex stability with Al^{3+} and the Al^{3+} coordination number was 6, forming the octahedral structure of d^2sp^3 miscellaneous. Ni^{2+} and Co^{2+} is dsp^2 miscellaneous chemical bond to form a flat tetrahedral structure. Thus, more octahedral particles have appeared for NCA-Citric acid (as shown in Figure 1 c1-c3), which will increase the diffusion path of lithium ions and is not conducive to electrochemical property [31].



Scheme 2. Effect of complexation reaction equilibrium factors.

4. CONCLUSIONS

In this paper, NCA cathodes have been prepared by sol-gel method. We have studied the influence of complexing agents (i.e. EDTA, glycine and citric acid) on the structures and morphologies of the resultant products. Experimental results show that although the NCA-EDTA, NCA-glycine, and NCA-citric acid samples prepared by different complexing agents all display the layered α - $NaFeO_2$ structures, their morphologies are completely different from each other. More single crystal octahedron can be found in the NCA-glycine and NCA-citric acid samples, but there is no any octahedron structure has been found in the NCA-EDTA. Electrochemical test results show that the NCA-EDTA

shows the maximum initial discharge capacity, the best charge-discharge cycle performance and the largest diffusion coefficients, which is due to the following factors: (1) EDTA shows the strongest complexing capacity, thus, EDTA and metal ions show the best complex stability and the NCA-EDTA particles can grow to perfect secondary particles. (2) As the super complex stability of EDTA and metal ions, the dissolve and re-crystallization processes become very weak, which will prevent the generation of octahedral structures for NCA-EDTA. (3) The resultant NCA-EDTA shows the largest lattice spacing and the best layer crystalline structure. All these advantages will make sure the largest initial discharge capacity, the best charge-discharge cycle performance and the largest diffusion coefficients of NCA-EDTA.

ACKNOWLEDGEMENTS

The authors gratefully acknowledge the financial support of the National Natural Science Foundation of China (No. 51364021 and 51264016).

References

1. J. B. Good enough and Y. Kim, *Chem. Mater.*, 22 (2010) 587-603.
2. T. Ohzuku and R. J. Brodd, *J. Power Sources.*, 174 (2007) 449-456.
3. W. Liu, P. Oh, X. Liu, M. J. Lee, W. Cho, S. Chae, Y. Kim and J. Cho, *Angewandte Chemie International Edition.*, 54 (2015) 4440-4457.
4. G. Hu, W. Liu, Z. Peng, K. Du and Y. Cao, *J. Power Sources.*, 198 (2012) 258-263.
5. Y. Kim, *Appl Mater. Interfaces.*, 4 (2012) 2329-2333.
6. C. J. Han, J. H. Yoon, W. I. Cho and H. Jang, *J. Power Sources.*, 136 (2004) 132-138.
7. G. T. K. Fey, R. F. Shiu, V. Subramanian, J. G. Chen and C. L. Chen, *J. Power Sources.*, 103 (2002) 265-272.
8. G. T. Kuo Fey, J. G. Chen, Z. F. Wang, H. Z. Yang and T. P. Kumar, *Mater Chem and Physics.*, 87 (2004) 246-255.
9. I. H. Son, J. H. Park, S. Kwon, J. Mun and J. W. Choi, *Chem. Mater.*, 27 (2015) 7370-7379.
10. Y. Kim and D. Kim, *Appl. Mater. Interfaces.*, 4 (2012) 586-589.
11. S. V. Lamaka, D. Höche, R. P. Petruskas, C. Blawert and M. L. Zheludkevich, *Electrochem Communications.*, 62 (2016) 5-8.
12. H. Liu, G. Zhu, L. Zhang, Q. Qu, M. Shen and H. Zheng, *J. Power Sources.*, 274 (2015) 1180-1187.
13. S. Watanabe, M. Kinoshita, T. Hosokawa, K. Morigaki and K. Nakura, *J. Power Sources.*, 258 (2014) 210-217.
14. Z. Wang, H. Liu, J. Wu, W. M. Lau, J. Mei, H. Liu and G. Liu, *RSC Advances.*, 6 (2016) 32365-32369.
15. Y. Zhou and H. Li, *J. Solid State Chem.*, 165 (2002) 247-253.
16. X.-J. Zhu, H.-X. Liu, X.-Y. Gan, M.-H. Cao, J. Zhou, W. Chen, Q. Xu, S.-X. Ouyang, *J. Electroceram.*, 17 (2006) 645-649.
17. S.B. Xia, Y.J. Zhang, P. Dong, Y.N. Zhang, *Eur. Phys. J.-Appl. Phys.*, 65 (2014) 10401.
18. K. Shizuka, C. Kiyohara, K. Shima, Y. Takeda, *J. Power Sources.*, 166 (2007) 233-238.
19. S.B. Majumder, S. Nieto, R.S. Katiyar, *J. Power Sources.*, 154 (2006) 262-267.
20. M. Xiang, W. Tao, J. Wu, Y. Wang, H. Liu, *Ionics* 22 (2016) 1003-1009.
21. H. Xie, G. Hu, K. Du, Z. Peng, Y. Cao, *J. Alloy. and Compd.*, 666 (2016) 84-87.

22. S.B. Xia, Y.J. Zhang, P. Dong, R.M. Yang, Y.N. Zhang, *Chinese J. Inorg. Chem.*, 30 (2014) 529-535.
23. S.B. Xia, Y.J. Zhang, P. Dong, Y.N. Zhang, *Eur. Phys. J.-Appl. Phys.*, 66 (2014) 30403.
24. Y. Xu, X. Li, Z. Wang, H. Guo, B. Huang, *Mater. Lett.*, 143 (2015) 151-154.
25. H. Wang, C. Lai, Y. Xiao, X. Ai, *Mater. Lett.*, 160 (2015) 250-254.
26. D. Jiang, L. Zhao, Y. Shao and D. Wang, *RSC Advances.*, 5 (2015) 40779-40784.
27. D. Zou, X. Chu and F. Wu, *Ceramics International.*, 39 (2013) 3585-3589.
28. A. E. Abdel Ghany, A. M. A. Hashem, H. A. M. Abuzeid, A. E. Eid, H. A. Bayoumi and C. M. Julien, *Ionics.*, 15 (2009) 49-59.
29. H. Xie, K. Du, G. Hu, J. Duan, Z. Peng, Z. Zhang and Y. Cao, *J. Mater. Chem A.*, 3 (2015) 20236-20243.
30. X. Li, Z. Xie, W. Liu, W. Ge, H. Wang and M. Qu, *Electrochimica Acta.*, 174 (2015) 1122-1130.
31. Y. Su, T. Hu, L. Tang, W. Weng, G. Han, N. Ma and P. Du, *Thin Solid Films.*, 558 (2014) 118-124.

© 2017 The Authors. Published by ESG (www.electrochemsci.org). This article is an open access article distributed under the terms and conditions of the Creative Commons Attribution license (<http://creativecommons.org/licenses/by/4.0/>).